RESEARCH ARTICLE

High-power femtosecond laser generation from an all-fiber linearly polarized chirped pulse amplifier

Tao Wang[iD], Can Li, Bo Ren[iD], Kun Guo, Jian Wu[iD], Jinyong Leng, and Pu Zhou[iD]

College of Advanced Interdisciplinary Studies, National University of Defense Technology, Changsha, China

(Received 26 September 2022; revised 15 December 2022; accepted 6 February 2023)

Abstract
An all-fiber high-power linearly polarized chirped pulse amplification (CPA) system is experimentally demonstrated. Through stretching the pulse duration to a full width of approximately 2 ns with two cascaded chirped fiber Bragg gratings (CFBGs), a maximum average output power of 612 W is achieved from a high-gain Yb-doped fiber that has a core diameter of 20 μm with a slope efficiency of approximately 68% at the repetition rate of 80 MHz. At the maximum output power, the polarization degree is 92.5% and the M^2 factor of the output beam quality is approximately 1.29; the slight performance degradations are attributed to the thermal effects in the main amplifier. By optimizing the B-integral of the amplifier and finely adjusting the higher-order dispersion of one of the CFBGs, the pulse width is compressed to 863 fs at the highest power with a compression efficiency of 72%, corresponding to a maximum compressed average power of 440.6 W, single pulse energy of 5.5 μJ and peak power of about 4.67 MW. To the best of our knowledge, this is the highest average power of a femtosecond laser directly generated from an all-fiber linearly polarized CPA system.

Keywords: chirped pulse amplification; femtosecond laser; fiber laser; high-power laser; ultrafast laser

1. Introduction

High-power ultrafast fiber lasers have broadband applications in both basic science and industrial fields[1–4]. Compared with solid-state lasers, fiber lasers have the advantages of good beam quality, high conversion efficiency, convenient thermal management, compact structure, flexible operation and long-time stability[5,6]. More importantly, ultrafast fiber lasers have the intrinsic merits of high repetition rate operation, which makes them attractive for applications such as high harmonic generation (HHG)[7], extreme-ultraviolet (XUV) radiation[8], and isolated attosecond pulses (IAPs)[9], thanks to the increased photon flux that can shorten the time for signal collection.

Nevertheless, limited by the small mode field area of the fiber and the relative long-distance transmission of pulses, the direct power scaling of ultrafast fiber lasers is hampered by serious nonlinear effects[10–12]. This limitation has been alleviated to a considerable extent by the exploiting of the well-known chirped pulse amplification (CPA) technology[13–15], with which the peak power of the laser pulse

can be significantly reduced through temporally stretching the pulse to the sub-nanosecond regime. At present, with the leveraging of large mode area (LMA) Yb-doped fibers (YDFs) with dedicated structure design for suppressing the higher-order mode contents and nonlinear effects[16–23], the average power of ultrafast lasers that are emitted from a single fiber has reached 830 W[16]. However, these LMA fibers are generally difficult to fusion splice, and spatial coupling of the laser signal is inevitable for constructing the high-power CPA system, of which the stability, flexibility and compactness would be highly compromised. However, for the all-fiber CPA system, owing to the utilization of a relatively small fiber diameter for fusion splicing and long transmission length for connection, the nonlinear effects are more severe and the corresponding progress in power scaling is lagging behind that of its free-space coupled counterpart. Although an all-fiber CPA system constructed by using YDF with a core/cladding diameter of 30/400 μm was demonstrated to generate an output power as high as 1052 W[24], the pulse was not temporally compressed at full power and there was considerable pedestal at the de-chirped pulse profile. In 2016, an all-fiber CPA laser based on YDF with a core/cladding diameter of 30/250 μm was reported to produce an average output power of 107 W, with a compressed pulse width of 566 fs and peak power

---

of 10.8 MW[25]. However, the output laser pulse was non-linearly polarized, rendering it less desirable for most applications. At the same year, our group utilized YDF with a core/cladding diameter of 30/250 μm to construct a linearly polarized CPA laser, and through optimizing the design of the fiber amplifier, femtosecond lasers with output powers of 119 W[26] and 300 W[27] were successively obtained. It is worth noting that the above-mentioned representative works on high-power all-fiber ultrafast lasers were carried out by using short length LMA YDF with a core diameter of 30 μm, which can effectively increase the threshold of nonlinear effects, whilst the system was still hindered by the mode degradation. In addition, it is well known that such large core fibers are prone to develop higher-order transverse mode contents under high-power operation even though the beam quality can be measured to be $M^2 < 1.2$, and this would be detrimental for specific applications when a coherent source is desirable[28]. In order to well balance the beam quality, output power, nonlinear effects and thermal load, employing a gain fiber with relatively medium mode field area, such as YDF with a diameter of 20 μm, combined with a large pulse width to mitigate the nonlinear effects, would be a good potential way to generate high-power ultrafast laser with an all-fiber configuration.

In this paper, we experimentally demonstrated a high-power all-fiber linearly polarized CPA system based on YDF with a core/cladding diameter of 20/400 μm. Through stretching the pulse width to a full width of 2 ns, a maximum output power of 612 W before pulse compression was

realized at a repetition rate of 80 MHz. Under the highest output power, the polarization degree of the laser pulse was measured to be 92.5%, whereas the M^2 factor of the collimated output beam was 1.29. The slight performance degradations were attributed to the thermal effects in the main amplifier, especially that in the fiber coupled collimator that integrated with the function of cladding mode stripping. By optimizing the B-integral and the high-order dispersion, the pulse duration could be compressed to 863 fs at the highest average power by a pair of diffraction gratings with line density of 1739 lines/mm. Under a compression efficiency of 72%, a maximum power of 440.6 W was obtained with a single pulse energy of 5.5 μJ and a peak power of up to 4.67 MW. To the best of our knowledge, this is the highest average power of a femtosecond laser realized from a single channel all-fiber linearly polarized CPA system ever reported. It should be noted that benefitting from the relatively small core of the main amplifier, no thermally induced transverse mode instability was observed during the power amplification and further power scaling is limited by the stimulated Raman scattering (SRS) effect and gain saturation.

2. Experimental setup

The experimental setup of the all-fiber high-power linearly polarized CPA system is presented in Figure 1. The seed laser was a semiconductor saturable absorption mirror (SESAM) based mode-locked fiber laser, which has a
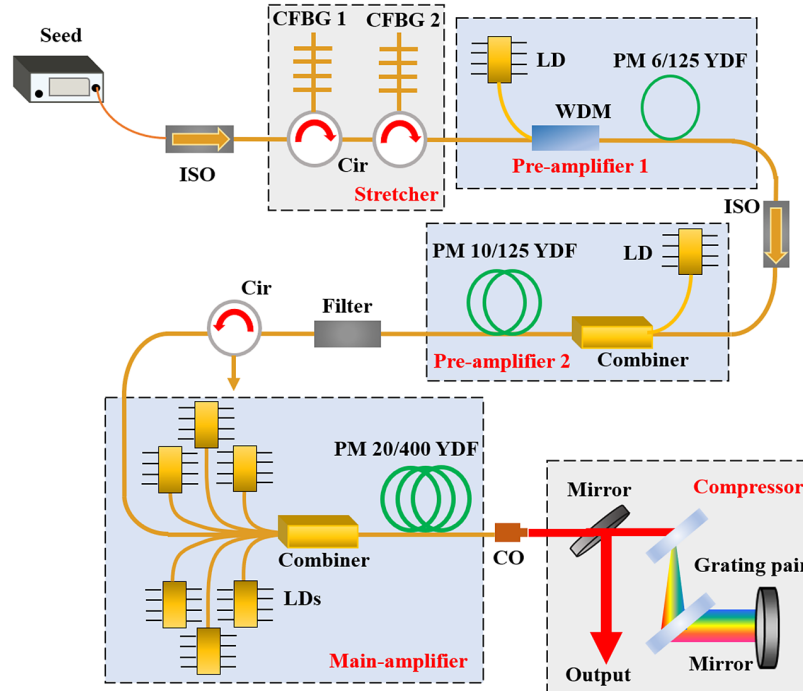

Figure 1. Experimental setup of the high-power linearly polarized CPA system. ISO, isolator; Cir, circulator; CFBG, chirped fiber Bragg grating; LD, laser diode; WDM, wavelength division multiplexer; PM YDF, polarization-maintaining Yb-doped fiber; CO, collimator.

repetition rate of 80 MHz and a pulse duration of 6 ps. After passing through an isolator (ISO), the seed laser was temporally stretched by two cascaded chirped fiber Bragg gratings (CFBGs), resulting in a highly chirped pulse with a full width of 2 ns. Both CFBG 1 and CFBG 2 have the central wavelength of 1030 nm, with 3-dB bandwidths of 15 and 11 nm, respectively. CFBG 1 can provide a group velocity dispersion (GVD) and a third-order dispersion (TOD) of 42.96 ps^2 and –0.66 ps^3, respectively. CFBG 2 can provide a GVD of 42.90 ps^2, whereas its TOD can be adjusted from –0.987 to –0.305 ps^3 through applying an electronically controlled stress. After that, the laser pulse was successively amplified by two pre-amplifiers and a main amplifier. Pre-amplifier 1 employed a piece of 3.5 m YDF with a core/cladding diameter of 6/125 μm, and was core-pumped by a 976 nm single mode laser diode (LD) via a wavelength division multiplexer (WDM). Pre-amplifier 2 used 1.3 m YDF with a core/cladding diameter of 10/125 μm, and was cladding-pumped by a multi-mode LD via a signal/pump combiner. After pre-amplifier 2, the power of the laser pulse was boosted to 10.8 W, and then the signal was injected into the main amplifier after passing through a filter and a circulator (Cir). The filter has a bandwidth of 10 nm and was used to reject the amplified spontaneous emission (ASE) produced during the pre-amplifications, whereas the circulator was employed to protect the front stages and monitor the backward scattered light. For the main amplifier, a YDF with a core/cladding diameter of 20/400 μm and high doping concentration was utilized to shorten the amplification length, for the sake of alleviating the nonlinear effects. Specifically, the cladding absorption coefficient of the YDF is 2.6 dB/m at 976 nm, the numerical apertures of the core and cladding are 0.07 and 0.48, respectively, and the actual length of the gain fiber is 4.5 m. The pump power was coupled into the YDF via a (6+1)×1 pump/signal combiner. The amplified laser pulse was output to the free space through a customized fiber collimator with the integrated function of cladding mode stripping. It is noted that the employment of the collimator is beneficial for flexible delivery; however, it has not been adopted in most of the previous works[25,29–32]. Finally, the collimated laser was compressed by a pair of transmission diffraction gratings (130 mm × 15 mm in size), of which the line density is 1739 lines/mm with a Littrow angle of 64°. A double-pass scheme was utilized to ensure a compact structure of the compressor.

3. Results and discussion

The seed laser has an output power of 76 mW and a center wavelength of 1030 nm with a 3 dB bandwidth of 9.97 nm, as shown in Figure 2(a) (0.02 nm spectral resolution for all the spectral measurement in this work). Figure 2(b) presents the pulse train of the seed laser; the corresponding repetition rate is 80 MHz and the pulse duration is around 6 ps. With the stretching of the CFBGs, the seed pulse was temporally broadened to 2 ns, with the detection by a 5 GHz photodetector and 1 GHz oscilloscope (as shown in Figure 3(b)), whereas the corresponding average power was reduced to 33.7 mW owing to the insertion loss of the CFBGs and circulators. The reflected spectrum after the two cascaded CFBGs is presented in Figure 3(a), demonstrating 3-dB and 10-dB bandwidths of 4.52 and 10.82 nm, respectively. The pulse power was successively amplified to 315 mW and 10.8 W by the pre-amplifiers, with the pulse duration slightly narrowed to a 3-dB width of 1.12 ns owing to mainly the saturation effect of pre-amplifier 2, as shown in Figure 3(b).

The output power of the main amplifier demonstrates a linear increasing trend with the increasing of the pump power, and no sign of power roll off was observed, as shown in Figure 4(a). The estimated slope efficiency was 68% and the maximum output power was 612 W under the pump power of 903 W, whereas further power scaling was hindered by the onset of gain saturation and SRS. In addition, during the laser performance characterization, the maximum average power is reproducible within ±5 W by repeating the
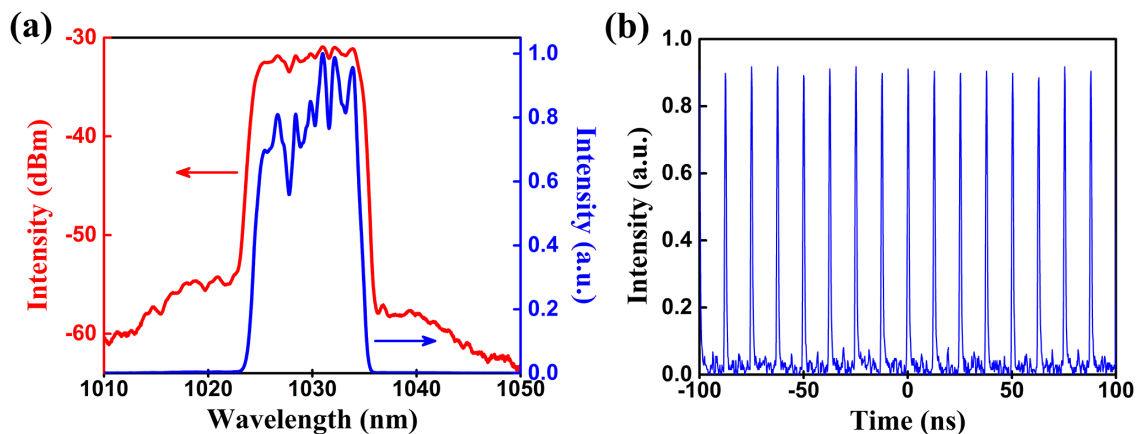

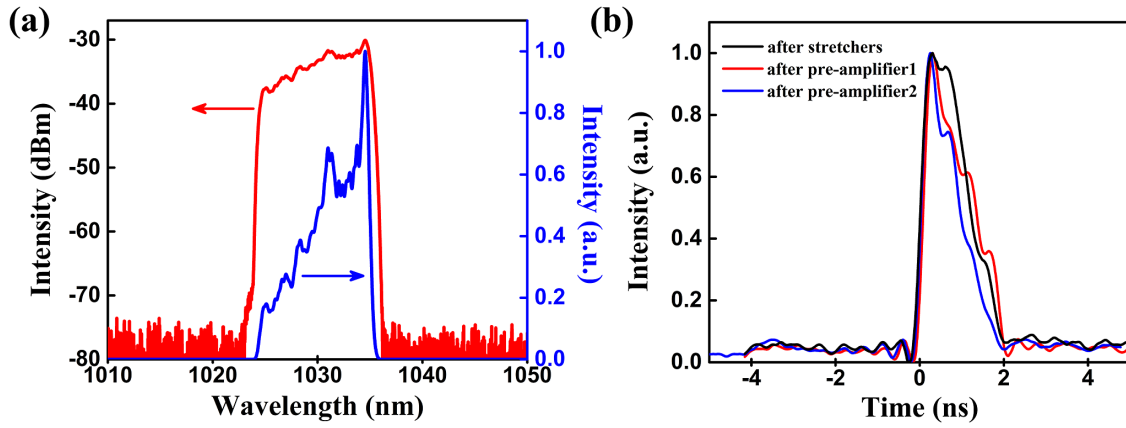**Figure 2.** The laser properties of the seed pulse: (a) output spectrum; (b) pulse train.

Figure 3. (a) Output spectrum after two cascaded CFBGs. (b) Pulse waveforms after the two cascaded CFBGs, pre-amplifier 1 and pre-amplifier 2.
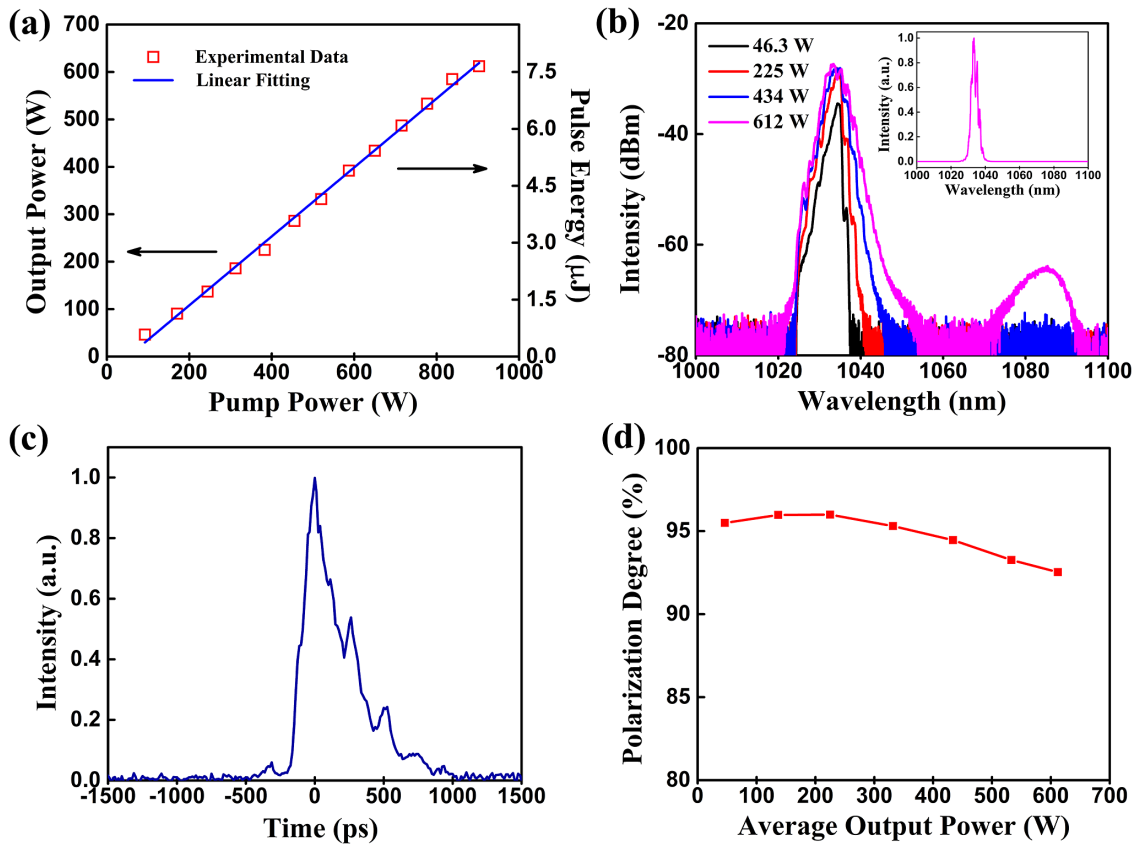

Figure 4. Output characteristics of the main amplifier: (a) average power and single pulse energy as a function of the pump power; (b) output spectra at selected output power; inset: linear-scale spectrum at the highest power; (c) pulse waveform at the highest power; (d) evolution of the polarization degree with the enhancement of the output power.

measurements. Also shown in Figure 4(a) is the corresponding evolution of the single pulse energy, and a maximum of 7.65 µJ was obtained. Figure 4(b) shows the optical spectra at different operation powers of the main amplifier. The inset is the corresponding linear-scale spectrum at the highest power. It can be seen that owing to the gain narrowing effect of the pre-amplifiers, the spectrum of the laser pulse was considerably narrowed, and the corresponding 3 dB bandwidth was measured to be 1.90 nm at the output power

of 46.3 W of the main amplifier. With the increasing pump power, a self-phase modulation-induced spectral broadening effect was observed, and at the maximum power the 3 and 10 dB bandwidths are 4.24 and 8.67 nm, respectively. In addition, at the output power of 612 W, the SRS component appeared at the wavelength of 1085 nm, and with an intensity of more than 36 dB weaker than that of the pulse signal, indicating that its influence on the laser performance is negligible. Figure 4(c) shows the temporal pulse waveform
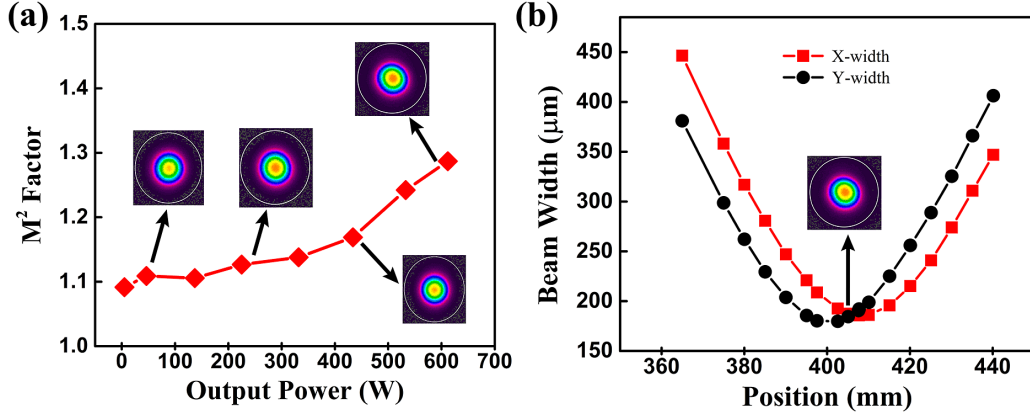
Figure 5. (a) Beam quality of the main amplifier at the selected operating power; (b) M^2 factor at the output power of 612 W.

at the highest power, and a typical gain saturation-induced narrowing effect can be observed, resulting in a 3 dB pulse width of 363 ps, with the detection by a high-speed photodetector and an oscilloscope with bandwidths of 45 and 36 GHz, respectively. In addition, the polarization degree of the output laser was investigated by using a $\lambda/2$ wavelength plate and a polarization beam splitter, and the results are presented in the Figure 4(d), in which the polarization degree is gradually decreased from 95.5% to 92.5% during the power enhancement progress, mostly owing to the thermally caused polarization degradation in the gain fiber.

Furthermore, the beam quality of the main amplifier was investigated in detail by a beam quality analyzer with the 4σ method, and the corresponding M^2 factors averaged in the x and y directions at selected operating powers are demonstrated in Figure 5(a). It can be seen that the M^2 of the collimated laser beam remains at around 1.1 with output power of less than 200 W, and it slightly degraded to 1.29 with the increasing power to 612 W, as shown in Figure 5(b). It is worth noting that in order to suppress higher-order modes, the gain fiber of the main amplifier was coiled to a diameter of about 10 cm and placed on a water-cooling plate. The deterioration of the beam quality at higher power is attributed to the higher mode stripping-induced temperature rising inside the customized fiber collimator, of which the structure design needs to be further optimized.

The nonlinearities experienced by the laser pulse during amplification directly affect the spectral and temporal performances and should be minimized[33,34]. Essentially, they can be quantified by the accumulated nonlinear phase shift in terms of the B-integral and can be calculated as follows:

$$B = \gamma P_0 \left\{ \left[\exp\left(g L_g \right) - 1 \right] / g + \exp\left(g L_g \right) L_p \right\},$$

where γ represents the nonlinear parameter, P_0 represents the peak power of the input signal, g represents the gain coefficient of fiber and L_g and L_p represent the length of the gain and the passive fiber, respectively[35]. It can be seen that an effective method to reduce the B-integral of

the main amplifier is shortening the corresponding lengths of the active and passive fibers, which have been optimized to 4.5 and 0.3 m (the pigtail of the collimator for delivery), respectively. Based on the actual experimental parameters, the calculated B-integrals of the pre-amplifiers are trivial, while that of the main amplifier is 1.64π radians at the operating power of 612 W. It should be noted that although the exponential approximation of the amplification profile along the active fiber may not accurately reflect the reality, it can still allow for a fairly good estimation of the exact B-integral and provide useful guidance for engineering the experimental system[27,32,33,35]. In this condition, through carefully adjusting the vertical distance of the compression gratings, the duration of the amplified pulse could be compressed to 1264 fs, assuming a Gaussian pulse envelope at the maximum output power, as shown in Figure 6(a). However, owing to the uncompensated higher-order dispersion that is induced by the nonlinear effects, there were satellite peaks presenting in the corresponding autocorrelation trace, indicating a considerable degradation of the pulse quality. This was partly addressed by finely adjusting the stress of one of the CFBGs to compensate for the higher-order dispersion, and the satellite peaks disappeared in the autocorrelation trace with the corresponding pulse duration shortened to 863 fs, as presented in Figure 6(b). In order to further shorten the pulse width, the pulse pre-chirping technique[17] would be adopted to compensate for the nonlinear phase that accumulated during the fiber amplification. In addition, the spectrum pre-shaping technique[36,37] or shifting the operation wavelength to avoid the gain peak of Yb emission[38] would be helpful for alleviating the gain narrowing effect, enabling the realization of wider spectrum and shorter compressed pulse width after amplification. In addition, the compression efficiency of the grating pair was measured to be approximately 72%, corresponding to a maximum compressed average power of 440.6 W and single pulse energy of 5.5 µJ. The energy contained in the pulse main lobe is calculated to be approximately 77.80%, corresponding to a peak power of approximately 4.67 MW.
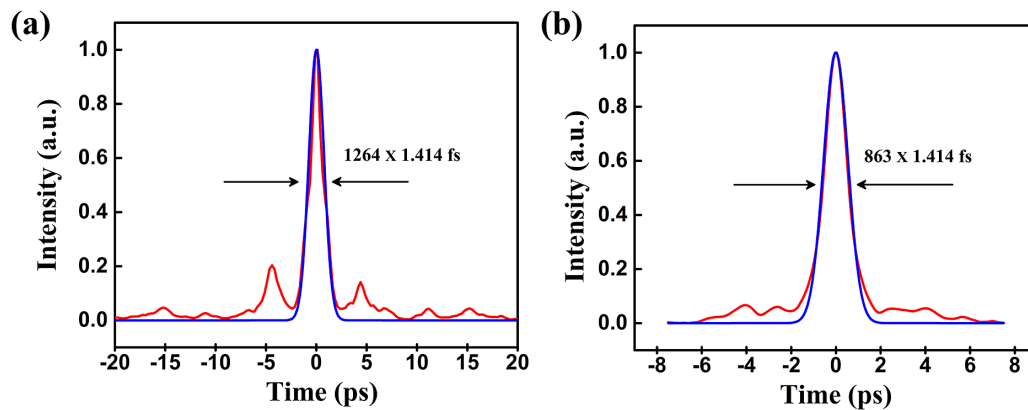
Figure 6. Autocorrelation traces of the compressed pulse at the highest output power (a) without and (b) with fine adjusting of the higher-order dispersion of the CFBG.

4. Conclusion

In conclusion, an all-fiber linearly polarized high-power ultrafast laser CPA system that employed a YDF with core diameter of 20 μm was experimentally demonstrated. Through temporally stretching the pulse duration to approximately 2 ns with two cascaded CFBGs, a maximum output power of 612 W was obtained with a slope efficiency of 68% at the repetition rate of 80 MHz. The polarization degree and beam quality at the highest power were measured to be 92.5% and $M^2 \sim 1.29$, respectively, and the slight degradations were attributed to the thermal effects in the customized collimator, for which a further optimized design is needed to realize a robust high-power ultrafast all-fiber laser system. In order to compensate for the higher-order dispersion that is induced by the nonlinear effects, one of the CFBGs was applied with electronically controlled stress to optimize the de-chirped pulse. A pulse duration of 863 fs was realized at the highest power with a compression efficiency of 72%, resulting in a record average power of 440.6 W with a single pulse energy of 5.5 μJ and a peak power of 4.67 MW. Compared with Ref. [27], the current work realized a significant increase of the output power with a smaller mode area and longer length of the main amplifier, indicating that a longer stretched pulse is very promising for scaling the output power of ultrafast lasers from an all-fiber CPA system. It is believed that this all-fiber, high-power, high repetition rate ultrafast laser could find broadband applications in material processing, ultrafast phenomenon detection, HHG and so on.

Acknowledgements

References

1. M. Malinauskas, A. Žukauskas, S. Hasegawa, Y. Hayasaki, V. Mizeikis, R. Buividas, and S. Juodkazis, Light Sci. Appl. **5**, e16133 (2016).
2. M. E. Fermann and I. Hartl, Nat. Photon. **7**, 868 (2013).
3. E. H. Penilla, L. F. Devia-Cruz, A. T. Wieg, P. Martinez-Torres, N. Cuando-Espitia, P. Sellappan, Y. Kodera, G. Aguilar, and J. E. Garay, Science **365**, 803 (2019).
4. N. Nishizawa, Jpn. J. Appl. Phys. **53**, 090101 (2014).
5. A. Tünnermann, T. Schreiber, and J. Limpert, Appl. Opt. **49**, F71 (2010).
6. G. Chang and Z. Wei, iScience **23**, 101101 (2020).
7. P. Ye, L. Gulyás Oldal, T. Csizmadia, Z. Filus, T. Grósz, P. Jójárt, I. Seres, Z. Bengery, B. Gilicze, S. Kahaly, K. Varjú, and B. Major, Ultrafast Sci. **2022**, 9823783 (2022).
8. A. Cingöz, D. C. Yost, T. K. Allison, A. Ruehl, M. E. Fermann, I. Hartl, and J. Ye, Nature **482**, 68 (2012).
9. M. Krebs, S. Hädrich, S. Demmler, J. Rothhardt, A. Zaïr, L. Chipperfield, J. Limpert, and A. Tünnermann, Nat. Photon. **7**, 555 (2013).
10. M. E. Fermann and I. Hartl, IEEE J. Sel. Top. Quantum Electron. **15**, 191 (2009).
11. E. Seise, A. Klenke, J. Limpert, and A. Tünnermann, Opt. Express **18**, 27827 (2010).
12. W. Fu, L. G. Wright, P. Sidorenko, S. Backus, and F. W. Wise, Opt. Express **26**, 9432 (2018).
13. D. Strickland and G. Mourou, Opt. Commun. **55**, 447 (1985).
14. M. L. Stock, A. Galvanauskas, M. E. Fermann, G. Mourou, and D. J. Harter, in *Nonlinear Guided-Wave Phenomena* (Optica Publishing Group, 1993), paper PD.5.
15. C. Gaida, M. Gebhardt, T. Heuermann, F. Stutzki, C. Jauregui, and J. Limpert, Opt. Lett. **43**, 5853 (2018).
16. T. Eidam, S. Hanf, E. Seise, T. V. Andersen, T. Gabler, C. Wirth, T. Schreiber, J. Limpert, and A. Tünnermann, Opt. Lett. **35**, 94 (2010).
17. Y. Liu, W. Li, D. Luo, D. Bai, C. Wang, and H. Zeng, Opt. Express **24**, 10939 (2016).
18. Q. Zhao, G. Gao, Z. Cong, Z. Zhang, G. Liu, Z. Liu, X. Zhang, and Z. Zhao, Opt. Express **30**, 3611 (2022).
19. W. Li, P. Ma, W. Lai, J. Song, T. Wang, B. Ren, W. Liu, P. Zhou, and L. Si, Opt. Laser Technol. **152**, 108166 (2022).
20. V. Filippov, Y. Chamorovskii, J. Kerttula, K. Golant, M. Pessa, and O. G. Okhotnikov, Opt. Express **16**, 1929 (2008).
21. J. Želudevičius, R. Danilevičius, K. Viskontas, N. Rusteika, and K. Regelskis, Opt. Express **21**, 5338 (2013).

22. F. Li, Z. Yang, Z. Lv, Y. Duan, N. Wang, Y. Yang, Q. Li, X. Yang, Y. Wang, and W. Zhao, Opt. Laser Technol. **129**, 106291 (2020).
23. Y. Zhang, R. Chen, H. Huang, Y. Liu, H. Teng, S. Fang, W. Liu, F. Kaertner, J. Wang, G. Chang, and Z. Wei, OSA Contin. **3**, 1988 (2020).
24. P. Wan, L.-M. Yang, and J. Liu, Opt. Express **21**, 29854 (2013).
25. R. Sun, D. Jin, F. Tan, S. Wei, C. Hong, J. Xu, J. Liu, and P. Wang, Opt. Express **24**, 22806 (2016).
26. H. Yu, P. Zhang, X. Wang, P. Zhou, and J. Chen, IEEE Photon. J. **8**, 7100507 (2016).
27. H. Yu, X. Wang, H. Zhang, R. Su, P. Zhou, and J. Chen, J. Light. Technol. **34**, 4271 (2016).
28. S. Wielandy, Opt. Express **15**, 15402 (2007).
29. S. Li, P. Li, K. Wang, N. Su, W. Xiong, and C. Yao, Appl. Phys. B **126**, 19 (2020).
30. F. Li, Z. Yang, W. Zhao, Q. Li, X. Zhang, X. Yang, W. Zhang, and Y. Wang, IEEE Photon. J. **8**, 1504206 (2016).
31. D. Deng, H. Zhang, Q. Gong, L. He, and J. Zu, IEEE Photon. J. **11**, 1505507 (2019).
32. F. Li, W. Zhao, Y. Wang, N. Wang, Q. Li, Y. Yang, and W. Wen, Opt. Laser Technol. **147**, 107684 (2022).
33. J. Limpert, F. Roser, D. N. Schimpf, E. Seise, T. Eidam, S. Hadrich, J. Rothhardt, C. J. Misas, and A. Tunnermann, IEEE J. Sel. Top. Quantum Electron. **15**, 159 (2009).
34. M. D. Perry, T. Ditmire, and B. C. Stuart, Opt. Lett. **19**, 2149 (1994).
35. G. P. Agrawal, *Nonlinear Fiber Optics* (Academic Press, 2013).
36. D. Nguyen, M. U. Piracha, and P. J. Delfyett, Opt. Lett. **37**, 4913 (2012).
37. C. Gu, Y. Chang, D. Zhang, J. Cheng, and S.-C. Chen, Opt. Lett. **40**, 4018 (2015).
38. D. N. Schimpf, J. Limpert, and A. Tünnermann, J. Opt. Soc. Am. B **27**, 2051 (2010).